Laser Light-Scattering Investigation of the Density of Pauci-Chain Polystyrene Microlatices

CHI WU* and KAM KWONG CHAN

Department of Chemistry, The Chinese University of Hong Kong, Shatin, N.T., Hong Kong

SYNOPSIS

The average density ($\langle\rho\rangle_{PCPS}$) of the pauci-chain polystyrene microlatices (PCPS), which contains a few linear polystyrene chains, was investigated by laser light scattering (LLS) including both angular dependence of absolute integrated scattered intensity (static LLS) and of the line-width distribution $G(\Gamma)$ (dynamic LLS). In static LLS, the weight-average particle mass (M_w) and the z-average radius of gyration (R_g) were measured; and simultaneously in dynamic LLS, the hydrodynamic radius distribution was obtained from Laplace inversion of very precisely measured intensity–intensity time correlation function. A combination of both the static and dynamic LLS results leads us to a value of $\langle\rho\rangle$. For comparison, we also determined $\langle\rho\rangle$ of conventional multichain polystyrene latex (MCPS) by following the same LLS procedure. It was found that $\langle\rho\rangle_{MCPS} = \langle\rho\rangle_{bulk} = 1.05$ g/cm^3, but $\langle\rho\rangle_{PCPS} = 0.92$ g/cm^3. This difference in density suggests that the intersegmental distance in MCPS or bulk polystyrene is smaller than that in PCPS, even the chains in PCPS are confined to a smaller volume. This might attribute to the fact, namely the intersegmental approaching inside PCPS is mainly the intrachain crossing which is more difficult in comparison with the interchain crossing inside MCPS or bulk polystyrene. © 1995 John Wiley & Sons, Inc.

Keywords: pauci-chain polystyrene microlatices • the density of pauci-chain microlatices • laser light scattering

INTRODUCTION

Pauci-chain polystyrene microlatices (PCPS), each contains only a few high-molecular weight polymer chains, can be made by the free radical polymerization of styrene in microemulsions.[1] In contrast to the formation of conventional multichain cross-linked polystyrene latex particles (MCPS) or bulk PS where the PS chain conformations are thermodynamically controlled, the PS chain conformations in PCPS are likely controlled by the formation kinetics.

Flory predicted that polymer chains in a bulk polymer have the same random coil conformations as in a Θ solvent.[2] Small-angle neutron scattering results have proven this prediction.[3,4] On average, a random coil chain in bulk polymer occupies only a few percent of its total accessible space. It has been shown that the random coil conformation requires the presence of the order of $\sim N^{1/2}$ interpenetrating chains (where N is the polymerization degree) to fill the available space.[5] $N^{1/2}$ can be as large as ~ 100 for polymer chains with high molecular mass.

For PCPS, the particle volume is considerably smaller than the accessible volume for a random coil chain in bulk polymer, which means that the polymer chain adopts a much highly compact conformation in the process of filling PCPS. Since the PS chains inside PCPS are packed in a quite different way, it would be interesting to find whether they are different in any way from bulk polymer. Qian et al.[6] showed that the compact globular form of polystyrene in PCPS at room temperature have a higher conformational temperature than that in bulk PS. They also showed that there is a dramatic difference between PCPS and bulk PS in the first run of DSC on the samples: namely, the existence of a first-order-like exothermic peak appeared

* To whom correspondence should be addressed.

Journal of Polymer Science: Part B: Polymer Physics, Vol. 33, 919–925 (1995)
 CCC 0887-6266/95/060919-07

around T_g for PCPS. They related this exothermic peak to the formation cohesional entanglements that is additional to the topological entanglements usually considered.[7]

Since the volume of a PCPS particle is much smaller than the accessible space of a given polymer chain with the random coil conformation in bulk polymer, it is usual to think at first sight that the average density of $\langle\rho\rangle_{PCPS}$ should be higher than $\langle\rho\rangle_{MCPS}$ or $\langle\rho\rangle_{bulk}$. However, after careful reconsideration, Qian[6] realized that this may not be true, since the accessible space of a polymer chain with the random coil conformation in bulk polymer contains on the order of $\sim N^{1/2}$ polymer chains while each PCPS particle contains only a few polymer chains. On the other hand, the intersegmental approaching inside PCPS is mainly from the *intrachain* crossing in contrast to that inside MCPS or bulk polymer mainly from the *interchain* crossing. The intrachain crossing should be more difficult than the interchain crossing because the polymer chain has a certain degree of rigidity, which indicates that the intersegmental distance in PCPS should be larger than that in MCPS or bulk polymer. Therefore, we should come to an opposite conclusion, namely, $\langle\rho\rangle_{PCPS}$ should be lower than $\langle\rho\rangle_{MCPS}$ or $\langle\rho\rangle_{bulk}$.

If true, this conclusion gives a new kind of polymer material which has a larger free volume. This larger free volume might be used in various applications, such as drug carrier and catalyst. The aim of this work was to determine the values of both $\langle\rho\rangle_{PCPS}$ and $\langle\rho\rangle_{MCPS}$ by a combination of static and dynamic laser light scattering (LLS) results. We will show that with proper experimental arrangement, a combination of static and dynamic LLS can provide a powerful tool in colloidal science.

BASIC THEORIES

Static Laser Light Scattering

The angular dependence of the excess absolute time-averaged scattered intensity, known as the excess Rayleigh ratio $[R_{vv}(\theta)]$, was measured. For a dilute solution at concentration C (g/mL) and the scattering angle θ, $R_{vv}(\theta)$ can be approximately expressed as[8]

$$\frac{KC}{R_{vv}(\theta)} \cong \frac{1}{M_w}\left(1 + \tfrac{1}{3}\langle R_g^2\rangle q^2\right) + 2A_2C \qquad (1)$$

where $K = 4\pi^2 n^2\left(\frac{dn}{dC}\right)^2 \Big/ (N_A\lambda_0^4)$ and $q = \frac{4\pi n}{\lambda_0}\sin\left(\frac{\theta}{2}\right)$

with N_A, dn/dC, n and λ_0 being Avogadro's number, the specific refractive index increment, the solvent refractive index, and the wavelength of light in vacuo, respectively. M_w is the weight average mass; A_2, the second-order virial coefficient; and $\langle R_g^2\rangle_z^{1/2}$, or simply as R_g, the root-mean-square z-average radius. By measuring $R_{vv}(\theta)$ at a set of C and θ, we can determine M_w, R_g, and A_2 from a Zimm plot which incorporates the dependence of $KC/R_{vv}(\theta)$ on both C and θ in a single grid.[8,9]

Dynamic Laser Light Scattering

An intensity-intensity time correlation function $G^{(2)}(t, \theta)$ in the self-beating mode is normally measured, which has the following form[9,10]

$$G^{(2)}(t, \theta) = \langle I(t, \theta)I(0, \theta)\rangle = A[1 + \beta|g^{(1)}(t, \theta)|^2] \qquad (2)$$

where A is a measured baseline; β, a parameter depending on the coherence of the detection; t, the delay time; and $g^{(1)}(t, \theta)$, the normalized first-order electric field time correlation function. $g^{(1)}(t, \theta)$ is related to the line-width distribution $G(\Gamma)$ by

$$g^{(1)}(t, \theta) = \langle E(t, \theta)E^*(0, \theta)\rangle = \int_0^\infty G(\Gamma)e^{-\Gamma t}\,d\Gamma \qquad (3)$$

The long accepted Laplace inversion program CONTIN[11] was used in this study to calculate $G(\Gamma)$ from $G^{(2)}(t, \theta)$. Normally, Γ is a function of both C and θ.[12] Γ is related to the translational diffusion coefficient D by $\Gamma = Dq^2$. D can be further converted to the hydrodynamic radius R_h by the Stokes-Einstein equation, $R_h = k_BT/(6\pi\eta D)$ where k_B, T, and η are the Boltzmann constant, the temperature (K), and the solvent viscosity, respectively.

EXPERIMENTAL

Sample Preparation

The PCPS microlatices were courtesy of Prof. Napper (School of Chemistry, The University of Sydney, Australia). The % wt/vol composition of the microemulsion for preparing the sample was: styrene 1.90; *n*-hexanol 0.95; cetyl trimethylammonium bromide (CTAB) 1.90; and water 95.25. The microemulsion was first prepared by titration at 60°C and then polymerized at 60°C by AIBN-initiated

polymerization for 20 h. The previous results showed that on average each PCPS particle contains about six linear PS chains ($M_w = 6.6 \times 10^5$ g/mol) which are quite uniform in length.[13] The conventional multichain polystyrene latex (MCPS) sample was purchased from Seradyn (Indianapolis, IN), wherein the stabilizer (surfactant) was cleaned-up by the ion-exchange procedure. The specified radius by the supplier is 22 nm and the particle density is 1.05 g/cm^3 which is the same as the density of bulk polystyrene. All solutions were prepared by successive diluting of a stock solution with known concentration.

Laser Light Scattering

A commercial LLS spectrometer (ALV/SP-125 with ALV-5000 multi-tau digital correlator, Langen in Hessen, Germany) was used with an argon-ion laser (Coherent INNOVA 90, operated at 488 nm and 100 mW) as light source. The laser beam is vertically polarized. In our present setup, the value of β in eq. (2) is ~ 0.85 which is rather high for an LLS spectrometer capable of doing both static and dynamic LLS measurements simultaneously, so that we are able to carry out dynamic LLS of very dilute solution. All LLS measurements were performed at 25.0 $\pm$ 0.1°C. The details of LLS can be found elsewhere.[9]

Specific Refractive Index Increment (dn/dC)

It is vital in static LLS to have a precise value of dn/dC. Recently, a novel differential refractometer was designed and constructed in our laboratory.[14] The whole refractometer mounted on a small optic rail is only 40 cm in length, 10 cm in width, and 15 cm in height, which can be easily incorporated into any existing LLS spectrometer, wherein the laser, the thermostat, and the computer are shared, which enables measurement of the refractive index increment and the scattered light intensity under the identical experimental conditions, such as wavelength and temperature.

RESULTS AND DISCUSSION

Our previous work proved that the accuracy and stability of the differential refractometer are so high that we are able to obtain the right dn/dC value just from one single-concentration measurement.[14] However, in order to get a more precise value of dn/dC, the Δn values of a set of four different concentrations, which ranges from 2×10^{-4} to 1×10^{-3} g/mL, were prepared and measured for PCPS and MCPS, respectively. For MCPS, the deionized water (< 0.5 μs) was used as solvent; and for PCPS, the deionized water with the same amount of stabilizer as in the microemulsion was used as solvent in order to account for the stabilizer in PCPS. In this way, the possible influence or effects of stabilizer on both the values of dn/dC and M_w have been removed experimentally. The measured dn/dC for MCPS in water is 0.256 $\pm$ 0.002 mL/g which is identical to the reported data,[15] but the measured dn/dC for PCPS is only 0.236 $\pm$ 0.002 mL/g, at $T = 25$°C and $\lambda = 488$ nm. According to the Lorentz-Lorentz equation or the Gladstone-Dale equation,[16] for a given homogeneous and unoriented polymer, the refractive index (n) should be proportional to its density (ρ), i.e., $n \propto \rho$, or further, $dn \propto d\rho$. The smaller dn/dC value of PCPS is in accord with a smaller density of PCPS, which implies that $\langle \rho \rangle_{PCPS}$ is ca. 8% lower than $\langle \rho \rangle_{MCPS}$. The static LLS results are summarized in Table I. The dependence of $[KC/R_{vv}(\theta)]_{\theta=0}$ on C, i.e., A_2, is negative, but practically zero (ca. -10^{-7} mol·mL/g^2) for both PCPS and MCPS.

Figure 1 shows two typical measured intensity-intensity time correlation functions of PCPS ("○", $C = 1.72 \times 10^{-4}$ g/mL) and MCPS ("□", $C = 2.14 \times 10^{-5}$ g/mL), where $\theta = 45°$. For samples with a narrow distribution, the measured correlation function can be analyzed by using either the Laplace inversion method first to obtain $G(\Gamma)$, and then, to calculate the z-average line width $\bar{\Gamma}$ ($= \int_0^\infty G(\Gamma)\Gamma d\Gamma$) and μ_2 ($= \int_0^\infty G(\Gamma)(\Gamma - \bar{\Gamma})^2 d\Gamma$), or the second-order Cumulants method to get $\bar{\Gamma}$ and μ_2 directly.[17]

Table I. Summary of Both Static and Dynamic LLS Results

Sample	dn/dC mL/g	M_w g/mol	R_g nm	$\bar{D}$ cm^2/s	$\bar{R}_h$ nm	$\mu_2/\bar{\Gamma}^2$	R_g/R_h
PCPS	0.236	4.2×10^6	12.5	1.53×10^{-7}	16.0	0.07	0.781
MCPS	0.256	2.9×10^7	17.1	1.04×10^{-7}	23.3	0.05	0.734

The relative errors: dn/dC, ±1%; M_w, ±3%; R_g, ±6%; D, ±1%.

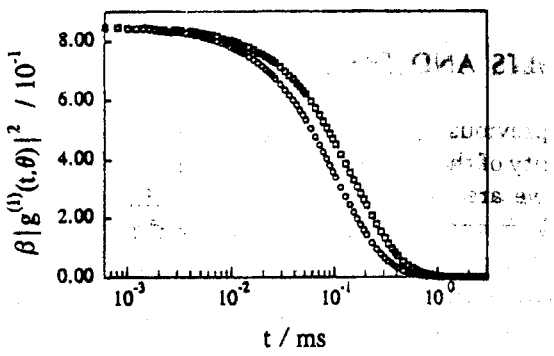

Figure 1. Typical measured intensity-intensity time correlation function of PCPS ("○", $C = 1.72 \times 10^{-4}$ g/mL) and MCPS ("□", $C = 2.14 \times 10^{-3}$ g/mL) at $\theta = 45°$ and $T = 25°C$.

These two methods produced essentially the same average results in the present study. Experimentally, we found that the measured $\bar{\Gamma}$ is independent of both C and θ. This is understandable since the particle size is relatively small and the solution was very dilute. As we mentioned before, Γ can be converted to D or R_h. The average values of $\bar{D}$ and $\bar{R}_h$ at $C = 0$ and $\theta = 0$ together with the values of $\mu_2/\bar{\Gamma}^2$ (the distribution width of $G(\Gamma)$) are also listed in Table I. If considering the larger experimental error associated with R_g, we found that the ratios of R_g to $\bar{R}_h$ for PCPS and MCPS reasonably agree with the theoretical value (0.77) predicted for a uniform hard sphere, which indicates that both the PCPS and MCPS particles are spheres with a uniform density. The values of R_g and $\bar{R}_h$ of PCPS in Table I are much smaller than the values (> 40 nm) of conventional polystyrene with a similar M_w in bulk state or in θ solvent,[18] which clearly shows that polystyrene chains inside PCPS are in a much compacted form.

Based on the data in Table I, for the first approximation, we calculated the apparent density $\rho_{app}(\bar{R}_h)$ of PCPS by replacing the molar mass M and R with M_W and $\bar{R}_h$, respectively, in the following density definition:

$$\rho = M/[N_A(4\pi/3)R^3] \qquad (4)$$

The calculated values of $\rho_{app,PCPS}$ and $\rho_{app,MCPS}$ are 0.403 g/cm^3 and 0.915 g/cm^3, respectively. They are quite different from each other and certainly lower than ρ_{MCPS} or ρ_{bulk} (=1.05 g/cm^3). According to the particle supplier, $\rho_{MCPS} = 1.05$ g/cm^3.

It is clear that eq. (4) is valid only for a monodisperse case. Even for a narrowly distributed sample, first, M_w and $\bar{R}_h$ are different from M and R; and second, M_w and $\bar{R}_h$ by their definitions have different averages. The difference between $\rho_{app,MCPS}$ and ρ_{MCPS} forced us to adopt a different way to calculate the particle density, wherein we started with $G(\Gamma)$ (or $G(D)$) instead of $\bar{\Gamma}$ (or $\bar{D}$), so that M and R instead of M_w and $\bar{R}_h$ were used.

Figure 2 shows two typical line-width distributions $G(D)$ of PCPS ("○") and MCPS ("□") obtained from the Laplace inversion of the time correlation functions presented in Figure 1. From these two distributions, we calculated $\langle D\rangle_z$, $\langle D\rangle_w$, and $\langle D\rangle_n$. For PCPS and MCPS, the ratios of $\langle D\rangle_z : \langle D\rangle_w : \langle D\rangle_n$ are 1.27 : 1.13 : 1.00, and 1.12 : 1.06 : 1.00, respectively, which show that both of them are narrowly distributed. However, PCPS is relatively broader than MCPS. The shapes of two distributions are slightly unsymmetrical toward the smaller D (i.e., toward the larger particles). It should be noted that $G(D)$ is an intensity-weighted distribution. Later on we will show that this slightly unsymmetrical portion of $G(D)$ in low D represents a long unsymmetrical tail in the number and weight distributions. According to the definition of $g^{(1)}(t)$, when $t \to 0$,

$$[g^{(1)}(t)]_{t\to 0} = \langle E(t)E^*(0)\rangle_{t\to 0} = \int_0^\infty G(\Gamma)\,d\Gamma \propto I \qquad (5)$$

On the other hand in the static LLS experiments, at $C = 0$ and $\theta = 0$, the net scattered intensity

$$I \propto \int_0^\infty f_w(M)M\,dM \propto \int_0^\infty f_n(M)M^2\,dM \qquad (6)$$

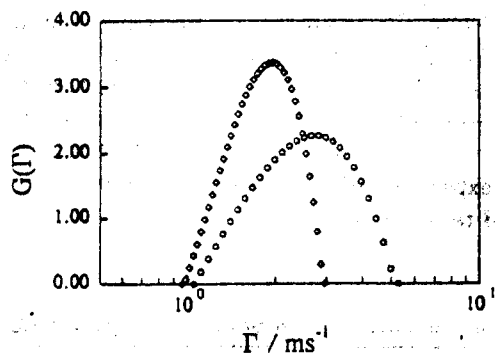

Figure 2. Typical line-width distribution $G(\Gamma)$ of PCPS ("○") and MCPS ("□") calculated from the Laplace inversion of the measured time correlation functions presented in Figure 1.

where $f_w(\propto f_n M)$ and f_n are the weight and number distributions, respectively. A comparison of eqs. (5) and (6) leads to

$$\int_o^\infty G(\Gamma)\, d\Gamma \propto \int_o^\infty f_n(M) M^2\, dM$$

or to

$$\int_o^\infty G(D)\, dD \propto \int_o^\infty f_n(M) M^2\, dM \qquad (7)$$

since $\Gamma = Dq^2$ and q is a constant for a given λ and θ. In the logarithmical space, eq. (7) can be rewritten as

$$\int_o^\infty G(D) D\, dln(D) \propto \int_o^\infty f_n(M) M^3\, dln(M) \qquad (8)$$

where $dln(M) \propto dln(R)$ and $dln(D) \propto dln(R_h)$ according to eq. (4) and the Stokes-Einstein equation, respectively, which leads to

$$\int_o^\infty G(D) D\, dln(D) \propto \int_o^\infty f_n(M) M^3\, dln(D) \qquad (9)$$

or

$$f_n(M) \propto G(D) D/M^3 \quad \text{and}$$

$$f_w(M) \propto G(D) D/M^2 \qquad (10)$$

Where $D \propto R_h^{-1}$. Therefore, in the logarithmical space, we have

$$f_n(R_h) \propto \frac{G(D)}{R_h^{10}} \propto G(D) D^{10} \quad \text{and}$$

$$f_w(R_h) \propto \frac{G(D)}{R_h^7} \propto G(D) D^7 \qquad (11)$$

where we have omitted all proportional constants since they are irrelevant to a given distribution. It can be seen that $f_n(R_h)$ is very sensitive to D. A slightly unsymmetrical in $G(D)$ will easily produce a profoundly unsymmetrical in f_n.

Figure 3 shows two number distributions of PCPS ("○") and MCPS ("□"). On the basis of these two distributions, we were able to calculate various hydrodynamic radii with different averages, such as $\langle R_h^2 \rangle_z^{1/2}$ and $\langle R_h \rangle_n$. These calculated average radii together with $\langle R \rangle_{TEM}$ from the calibrated transmission electron microscopy (TEM) are listed in Table II. From the nature of TEM experiment, we know that $\langle R \rangle_{TEM}$ was the number-average radius. This may explain why the values of $\langle R_h \rangle_n$ for both PCPS and MCPS are close to their corresponding values of $\langle R \rangle_{TEM}$. It can be seen that $\bar{R}_h$ is quite different from $\langle R \rangle_{TEM}$, even for the narrowly distributed PCPS and MCPS samples. In the past, this difference has been overlooked because it is not very critical to most applications, or in some cases, interpreted solely as the hydrodynamic effect or as the layer thickness of stabilizer (surfactant) adsorbed on the particle surface. Our LLS results clearly indicate that this difference is also caused by the different averages in different experimental methods. The broader the distribution, the larger the difference will be.

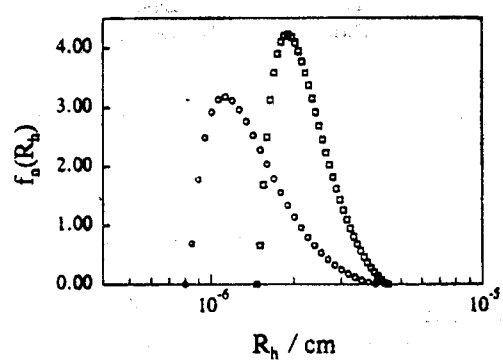

Figure 3. Number distributions $f_n(R_h)$ of PCPS ("○") and MCPS ("□"). The calculated different average hydrodynamic radii, i.e., $\langle R_h^2 \rangle_z^{1/2}$ and $\langle R_h \rangle_n$, are listed in Table II.

Table II also shows that for PCPS the difference between $\langle R_h \rangle_n$ and $\langle R \rangle_{TEM}$ is 1.9 nm. This difference is less than the geometric stretched length of the stabilizers (ca. 2.7 nm), which is reasonable and has been discussed before.[19] As for MCPS where the stabilizers have been washed out, $\langle R_h \rangle_n$ equals $\langle R \rangle_{TEM}$ within the experimental uncertainties. In order to have an estimation of the layer thickness of the stabilizer, we dialyzed the PCPS sample in deionized water to remove the stabilizer adsorbed on the surface of microlatices.

Figure 4 shows two number distributions of the hydrodynamic radius for the PCPS sample before and after the dialysis, by "○" and "□," respectively. After the dialysis the hydrodynamic radius distribution shifts toward the small size range, but the shape of the distribution remains. This is reasonable since dialysis only changes the hydrodynamic size of the particles, but does not alter the number of

Table II. Comparison of the Hydrodynamic Radius Measured or Calculated by Using Different Methods or Averages

Sample	$\bar{R}_h$	$\langle R_h^2 \rangle_z^{1/2}$	$\langle R_h \rangle_n$	$\langle R \rangle_{n,\mathrm{TEM}}$
PCPS	16.0	18.1	14.2	12.3 (nm)
MCPS	23.3	25.4	22.4	22.1 (nm)

The relative errors: $\langle R_h^2 \rangle_z^{1/2}$ & $\langle R_h \rangle_n$, ±3%; $\langle R \rangle_{\mathrm{TEM}}$, ±5%.

each fraction inside the distribution. From these distributions, we calculated the number-average hydrodynamic radius $\langle R_h \rangle_n$ at each dialysis stage.

Figure 5 shows a plot of $\langle R_h \rangle_n$ vs. t (the dialysis time). It clearly shows that $\langle R_h \rangle_n$ decreases as t increases and approaches to a constant value of 12.3 ± 0.1 nm, which is close to the value of $\langle R \rangle_{\mathrm{TEM}}$. Therefore, the number-average radius of the PCPS core should be close to this constant value of 12.3 nm. On the basis of eqs. (4) and (11), we can calculate the weight-average molar mass ($M_{w,\mathrm{cal}}$) from $f_w(M)$ for both PCPS and MCPS according to the definition of M_w,

$$M_{w,\mathrm{cal}} = \int_o^\infty f_w(M) M \, dM \Big/ \int_o^\infty f_w(M) \, dM$$

$$= \int_o^\infty f_w(M) M^2 \, d\ln(M) \Big/ \int_o^\infty f_w(M) M \, d\ln(M)$$

$$= \left(\frac{4}{3}\pi\rho N_A\right) \cdot \left(\frac{6\pi\eta}{k_B T}\right)^3 \times \frac{\int_o^\infty G(D) D \, d\ln(D)}{\int_o^\infty G(D) D^4 \, d\ln(D)} \quad (12)$$

where we have changed M to R_h, and then, R_h to D. ρ is the only unknown parameter on the right side and the rest can be obtained from $G(D)$. For a given particle system, $M_{w,\mathrm{cal}}$ should be equal to the measured M_w from static LLS, or in other words, $M_{w,\mathrm{cal}}$ can be replaced by M_w [i.e., M_w can be used as a constraint in eq. (12)]. On the basis of eq. (12), the density ρ can be calculated from a combination of static and dynamic LLS results (i.e., M_w from static LLS and $G(D)$ from dynamic LLS).

Such calculated values of ρ_{PCPS} and ρ_{MCPS} are 0.92 and 1.05 g/cm^3, respectively. On the one hand, for MCPS, the agreement between ρ_{MCPS} and ρ_{MCPS} (supplier) or ρ_{bulk} shows that the method used in this study is proper for the evaluation of the particle density; on the other hand, for PCPS, it confirms that ρ_{PCPS} is lower than that of MCPS or bulk PS. This lower value of ρ_{PCPS} is supported by the porosimetry measurement of the harvested PCPS microlatices, where the density of PCPS is ca. 9.5% lower than that of MCPS.[13] We might attribute this lower density to the fact, in PCPS, that the intersegmental crossing happens mainly within one polystyrene chain (i.e., mainly the intrachain crossing), since there are only a few chains inside each PCPS particle, while in MCPS, the interchain crossing will be dominant. Because the PS chain has a certain degree of rigidity, the intrachain crossing should be more difficult in comparison with the interchain

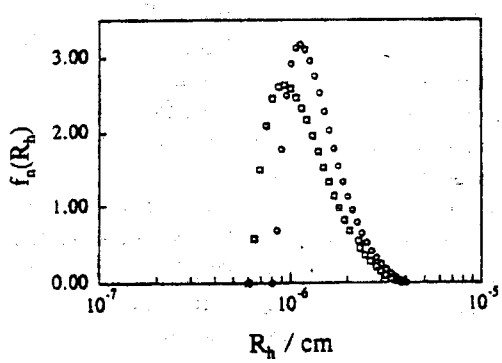

Figure 4. Two number distributions of the hydrodynamic radius for the PCPS sample before and after the dialysis, represented by "○" and "□," respectively.

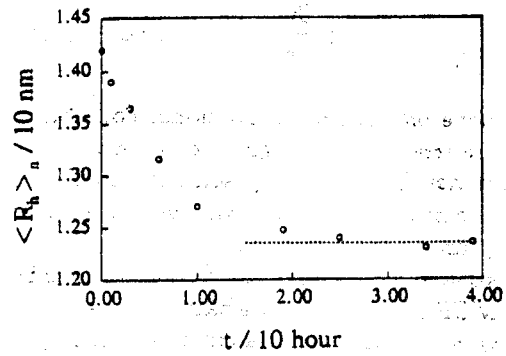

Figure 5. Plot of the number-average hydrodynamic radius $\langle R_h \rangle_n$ vs. the dialysis time t. The dotted line shows an approaching value of $\langle R_h \rangle_n$ at infinite dialysis time.

crossing. Thus, the intersegmental distance in PCPS should be larger than that in MCPS, which leads to a lower density.

CONCLUSIONS

The characterization of pauci-chain polystyrene microlatices (PCPS) has been accomplished by using a combination of static and dynamic laser light scattering results. Both the specific refractive index increment dn/dC and the calculated density values suggest that PCPS prepared by free radical polymerization of styrene in microemulsions has a lower density in comparison with conventional latices made of cross-linked polystyrene chains (MCPS) or bulk polystyrene. This density difference implies that, on average, the intersegmental distance between a few chains in PCPS is slightly larger than the intersegmental distance between many different chains in bulk polystyrene or in MCPS, or in other words, the free volume inside PCPS is larger than that in MCPS. The importance of this less packed nature of PCPS remains to be explored.

The authors are indebted to Prof. Napper, D. H. and Ms. Tan, G. (The University of Sydney, Australia) for providing the PCPS sample, and to Prof. Qian (The Institute of Chemistry, Beijing, China) for initiating this study. The financial support of this work by the RGC (the Research Grants Council of Hong Kong Government) Earmarked Grant 1993/94 (CUHK 79/93E, 221600140) is gratefully acknowledged.

REFERENCES AND NOTES

1. J. S. Guo, M. S. El-Aasser, and J. W. Vanderhoff, *J. Polym. Sci. Polym. Chem. Ed.*, **27**, 691 (1989).
2. P. J. Flory, *Principles of Polymer Chemistry*, Cornell University Press, Ithaca, NY, 1953.
3. R. G. Kirste, W. A. Kruse, and J. Scheltens, *Makromol. Chem.*, **162**, 299 (1973).
4. J. P. Cotton, D. Decker, H. Benoit, B. Farnoux, J. Higgins, G. Jannink, R. Ober, C. Picot, and J. des Cloizeaux, *Macromolecules*, **7**, 863 (1974).
5. P-G. de Gennes, *Scaling Concepts in Polymer Physics*, Cornell University, Ithaca, NY, 1979, Chap. 2.
6. R. Qian, L. Wu, D. Shen, D. H. Napper, R. A. Mann, and D. F. S. Sangster, *Macromolecules*, accepted for publication.
7. R. Qian, *Abstr. China-UK Bilateral Conference on Polymer Science*, Beijing, April 1992, p. 2.
8. B. H. Zimm, *J. Chem. Phys.*, **16**, 1099 (1948).
9. B. Chu, *Laser Light Scattering*, Academic Press, New York, 1974.
10. R. Pecora, *Dynamic Light Scattering*, Plenum Press, New York, 1976.
11. S. W. Provencher, *Biophys. J.*, **16**, 29 (1976); *J. Chem. Phys.*, **64**, 2772 (1976); *Makromol. Chem.*, **180**, 201 (1979).
12. W. H. Stockmayer and M. Schmidt, *Pure. Appl. Chem.*, **54**, 407 (1982); *Macromolecules*, **17**, 509 (1984).
13. R. Qian and D. H. Napper, private communication, the results have been submitted to *Macromolecules* for publication.
14. C. Wu and K. Q. Xia, *Rev. Sci. Instrum.*, **65**(3), 587 (1994).
15. F. S. Chan and D. A. I. Coring, *Can. J. Chem.*, **44**, 725 (1966).
16. G. Gee, *Polymer*, **7**, 177 (1966).
17. D. E. Koppel, *J. Chem. Phys.*, **57**, 4814 (1972).
18. H. Fujita, *Macromolecules*, **21**, 179 (1988).
19. C. Wu, *Macromolecules*, **27**, 298 (1994).

Received June 23, 1994
Revised October 31, 1994
Accepted November 2, 1994